An aza-cyclophane stacked in racemic columnar assemblies: whole-molecule disorder in a two-dimensional solid solution

Matthias Zeller,[a]* Marlon R. Lutz Jr[b] and Daniel P. Becker[b]

[a]Youngstown State University, Department of Chemistry, 1 University Plaza, Youngstown, OH 44555-3663, USA, and [b]Department of Chemistry, Loyola University, 6525 North Sheridan Road, Chicago, IL 60626, USA

Correspondence e-mail: mzeller@cc.ysu.edu

The oxime derivative of [1.1.1]cyclophane cyclotriveratrylene (CTV) was ring expanded utilizing a Beckmann rearrangement to provide a ten-membered N-acetyl macrocyclic amide that crystallizes as a chloroform monosolvate in columnar assemblies manifesting an unusual disorder within the crystal. Columns made up of this structure consist of infinite columnar assemblies of alternating D and L enantiomers and therefore necessarily are made up of a racemate, yet the chiralities of individual molecules in adjacent columns are independent of one another, leading to the overall formation of a two-dimensional solid solution. The random arrangement of the columns within the structure leads to the emergence of a crystallographic mirror plane not reflected by the molecular symmetry, to a change of symmetry from $Pna2_1$ to $Pnma$ and to whole-molecule disorder of the bowl-shaped molecules within the columns.

1. Origin of the material

Cyclotriveratrylene (CTV; Collet, 1987) and its [1.1.1]cyclophane congeners in their rigid crown conformation are unique bowl-shaped molecules that serve as supramolecular scaffolds, and they can function as molecular receptors utilizing their concave face for the recognition of suitable small molecules (Collet, 1996; Burlinson & Ripmeester, 1984; Steed *et al.*, 1996). Our interest in the crown-saddle conformational interconversion of CTV derivatives including CTV oxime [$1^4,1^5,3^4,3^5,5^4,5^5$-hexamethoxy-1,3,5(1,2)-tribenzenacyclohexaphan-2-one oxime (1); Lutz, French *et al.*, 2007] led us to explore the Beckman rearrangement of this molecule (Lutz, Zeller & Becker, 2007). The Beckmann ring expansion (see below and §2) leads to an amide-containing concave 'pinched-bowl'-shaped, planar chiral azacyclophane with potential applications in host–guest chemistry, so we pursued the crystal structure of the N-acetyl macrocyclic amide [6-acetyl-$1^4,1^5,3^4,3^5,5^4,5^5$-hexamethoxy-6-aza-1,3,5(1,2)-tribenzenacycloheptaphan-7-one (2)].
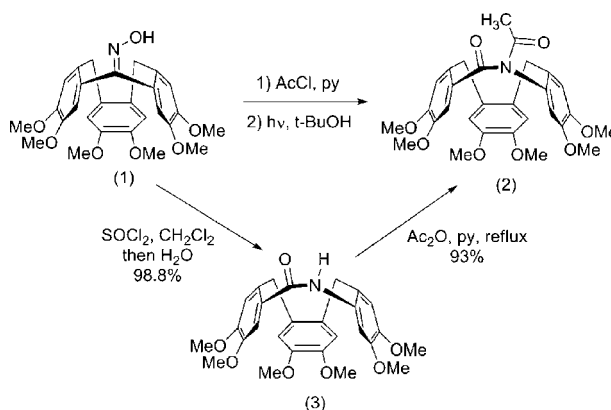
2. Experimental

2.1. Sample preparation

2.1.1. 6-Acetyl-1^4,1^5,3^4,3^5,5^4,5^5-hexamethoxy-6-aza-1,3,5(1,2)-tribenzenacycloheptaphan-7-one (2), method A.

To a solution of cyclotriveratrylene (CTV) oxime (1.00 g, 2.08 mmol; Lutz, French *et al.*, 2007), as a *ca* 1:1 mixture of crown and saddle conformers in pyridine (2.1 ml) at room temperature under an atmosphere of argon, was added acetyl chloride (0.246 g, 26.1 mmol) dropwise *via* a syringe. After 21 h at room temperature the orange–red reaction suspension was diluted with methylene chloride (20 ml) and washed successively with 1 N HCl (2 × 30 ml), saturated aqueous NaHCO$_3$ (20 ml), brine and then dried over sodium sulfate. Concentration gave the desired CTV oxime *O*-acetate intermediate (1.03 g, 95.1%) as a light orange foam which was a *ca* 1:1 mixture of saddle and crown conformers based on TLC. To a 50 ml Pyrex round-bottom flask that was flame-dried and charged with argon was added the cyclotriveratrylene oxime *O*-acetate (113 mg, 0.217 mmol) and 21.7 ml of *t*-butanol. This mixture was deoxygenated by placing the flask in a sonicator for 20 min with an argon purge. Under an argon atmosphere, the reaction mixture was then irradiated with a 400 W mercury lamp at room temperature for 3 h. Removal of solvent under reduced pressure gave 115 mg of an orange residue. Purification *via* chromatography gave the Beckmann amide *N*-acetate product (2) as a colorless solid (20.4 mg, 18%). Crystals were grown by diluting 20 mg of (2) in 0.5 ml of CDCl$_3$ with 5.0 ml of dichloromethane and 1.0 ml of hexane: m.p. 389–391 K (sintering only) following by melting at 405–408 K and subsequent effervescence, then resolidification at 413 K; a second melting point was then observed at 448–451 K. ^{1}H NMR (CDCl$_3$): δ 8.32 (1H, s, CHCl$_3$), 6.84 (1H, s), 6.82 (1H, s), 6.62 (1H, s), 6.59 (2H, s), 6.41 (1H, s), 4.25 (1H, d, 14.7 Hz), 4.01 (1H, s, 14.7 Hz), 3.92 (3H, s), 3.90 (3H, s), 3.77 (3H, s), 3.75 (3H, s), 3.73 (3H, s), 3.73 (3H, s), 3.72 (3H, s), 3.62 (1H, d, 14.7 Hz), 3.47 (1H, d, 14.7 Hz), 2.74 (3H, s). ^{1}H NMR (DMSO-d_6): δ 7.15 (1H, s), 7.13 (1H, s), 6.98 (1H, s), 6.94 (1H, s), 6.74 (1H, s), 6.72 (1H, s) 4.05 (1H, d, 14.0 Hz), 3.87 (1H, d, 14.0 Hz), 3.79 (3H, s), 3.78 (3H, s), 3.63 (3H, s), 3.62 (3H, s), 3.61 (3H, s), 3.60 (3H, s), 3.42 (2H, d, 14.6 Hz), 2.70 (3H, s).

(2)
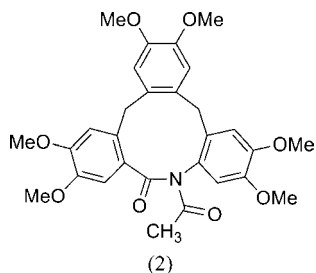
2.1.2. 6-Acetyl-1^4,1^5,3^4,3^5,5^4,5^5-hexamethoxy-6-aza-1,3,5(1,2)-tribenzenacycloheptaphan-7-one (2), method B.

To a solution of 1^4,1^5,3^4,3^5,5^4,5^5-hexamethoxy-6-aza-1,3,5(1,2)-tribenzenacycloheptaphan-7-one (3) (100 mg,

0.209 mmol; Lutz *et al.*, 2008) in pyridine (1.0 ml) was added acetic anhydride (0.5 ml), and the mixture was heated to reflux for 2 h. After cooling to room temperature the reaction mixture was diluted with deionized water (18 ml) to give a slurry which was extracted with ethyl acetate (3 × 5 ml). The combined organic layers were successively washed with 1M aqueous HCl (2 × 10 ml), deionized water (1 × 10 ml) and brine (1 × 10 ml), and dried over sodium sulfate. Concentration under reduced pressure afforded 121 mg of a golden yellow glass. Column chromatography eluting with a gradient (100% CH$_2$Cl$_2$ to 35/65 diethyl ether/CH$_2$Cl$_2$) with a 28:1 loading ratio of silica gel afforded the *N*-acyl amide (2) (103 mg, 94.6%). Crystallization from either CDCl$_3$/CH$_2$Cl$_2$/hexane, CHCl$_3$/CH$_2$Cl$_2$/hexane or CHCl$_3$/hexane gave crystals that were identical by ^{1}H NMR to material prepared *via* method A, and with identical melting characteristics as described above.

2.2. Single-crystal data collection

2.2.1. Experimental strategy and data collection. Single-crystal X-ray data were collected on a Bruker AXS Smart

Table 1
Experimental details.

Crystal data	
Chemical formula	C$_{29}$H$_{31}$NO$_8$·CHCl$_3$
M_r	640.92
Cell setting, space group	Orthorhombic, *Pnma*
Temperature (K)	100 (2)
a, b, c (Å)	16.7247 (18), 15.7070 (16), 11.2154 (11)
V (Å^3)	2946.2 (5)
Z	4
D_x (Mg m^{-3})	1.445
Radiation type	Mo $K\alpha$
μ (mm^{-1})	0.36
Crystal form, colour	Plate, yellow
Crystal size (mm)	0.60 × 0.60 × 0.27
Data collection	
Diffractometer	Bruker AXS SMART APEX CCD
Data collection method	ω scans
Absorption correction	Multi-scan (based on symmetry-related measurements)
T_{min}	0.768
T_{max}	0.906
No. of measured, independent and observed reflections	19 031, 3783, 2924
Criterion for observed reflections	$I > 2\sigma(I)$
R_{int}	0.031
θ_{max} ($^\circ$)	28.3
Refinement	
Refinement on	F^2
$R[F^2 > 2\sigma(F^2)]$, $wR(F^2)$, S	0.077, 0.222, 1.04
No. of reflections	3783
No. of parameters	310
H-atom treatment	Constrained to parent site
Weighting scheme	$w = 1/[\sigma^2(F_o^2) + (0.0991P)^2 + 5.3522P]$, where $P = (F_o^2 + 2F_c^2)/3$
$(\Delta/\sigma)_{max}$	< 0.0001
$\Delta\rho_{max}$, $\Delta\rho_{min}$ (e Å^{-3})	0.96, −0.95

Computer programs used: *APEX2* v2.1–4 (Bruker, 2007), *SHELXTL* 6.14 (Bruker, 2000–2003; Sheldrick, 2008).
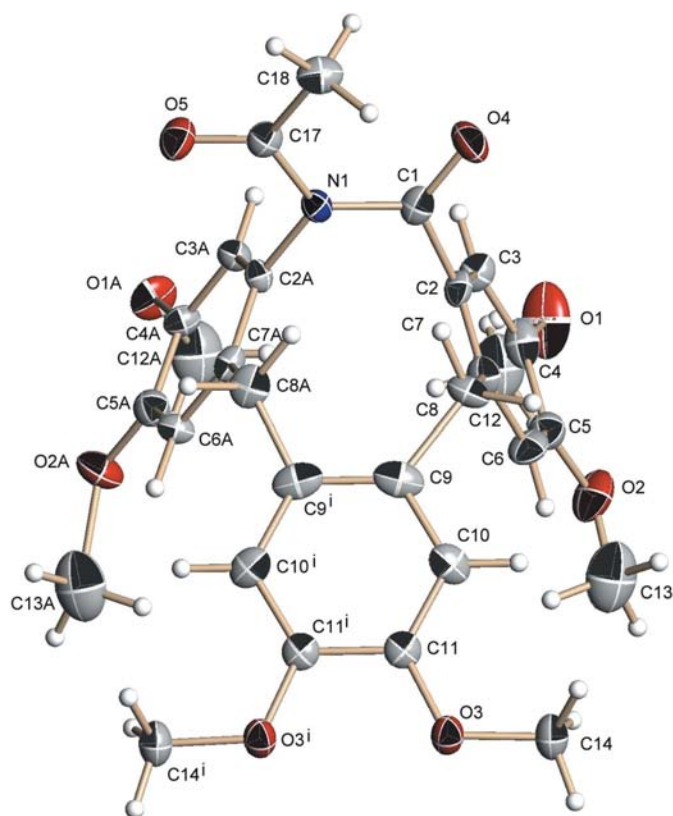
Figure 1
ORTEP-style representation of one symmetry-expanded molecule. Only one of the two possible molecules created by the whole-molecule disorder is shown and the chloroform solvate molecule is omitted for clarity. Symmetry code: (i) $x, \frac{1}{2} - y, z$; the probability of the displacement ellipsoids is set to 50%; H atoms are drawn at fixed arbitrary radii.

Apex diffractometer equipped with a Kryoflex cooling system using monochromatic Mo $K\alpha$ radiation with the ω-scan technique. A clear and perfectly transparent light-yellow plate without any obvious breaks or discontinuities was selected and mounted with the help of a small amount of mineral oil onto a MiTeGen MicroMesh mount with 25 µm mesh size. Experimental details are given in Table 1.

2.2.2. Crystal structure refinement. The molecule – while itself being planar, chiral and not mirror-symmetric – is located in the solid state on a crystallographic mirror plane, thus superimposing the image and mirror image of the molecule in a 1:1 ratio atop of each other. The main difference in steric demand between the two enantiomers is found in the *N*-acetylamide part of the macrocycle. The different steric demands of the *N*-acetyl *versus* the keto groups induce a noticeable shift of most of the atoms of the molecule when compared with their counterparts in the other enantiomer and only the dimethoxy benzene unit furthest away from the *N*-acetylamide exhibits exact mirror symmetry. The remainder of the molecule is disordered over two alternative sets of positions. The chloroform solvate molecule, also located on the mirror plane, shows no disorder. The positions of all the atoms in both the slightly shifted moieties are sufficiently well defined to allow for a refinement without any positional or similarity restraints. Displacement parameters of disordered

atoms are also well defined. Three pairs of mirror-related atoms with rather large overlap (C5 and C5*A*, C12 and C12*A*, and C13 and C13*A*) were constrained to have identical anisotropic displacement parameters (ADPs), but no other constraints or restraints were applied for any other atom in the structure. H atoms were added in calculated positions with C—H distances of 0.95, 0.99 and 0.98 Å for aromatic, methylene and methyl H atoms, respectively, and were refined with $U_{iso}(H) = x U_{eq}(C)$ (x = 1.2 for C—H and CH_2, 1.5 for CH_3).

The structure was also tentatively refined with the omission of the mirror plane perpendicular to the *b* axis in the alternative space group *Pna*2_1. However, the refinement resulted in a structure showing the same disorder as in *Pnma* with a 1:1 ratio for both moieties.[1] Inclusion of racemic twinning did not improve the structural model and the batch scale factor refined to 0.41 (19).

2.3. Differential scanning calorimetry (DSC), thermogravimetric analysis (TGA) and NMR spectroscopy

DSC data were collected on a 2910 differential scanning calorimeter, and TGA data were collected on a 2050 thermographimetric analyzer. Both instruments are from TA Instruments. DSC data were collected in sealed aluminum pans and TGA data in open aluminium pans. Heating rates were between 0.5 and 5 K per minute. The DSC of the *N*-acetyl derivative (2) reveals two separate endothermic events. The first endotherm begins at 405 K, consistent with melting of the crystal, observed in an open capillary using an Electrothermal Mel-Temp at 405–408 K, and then reaches the crest of a large heat influx at 421 K which is consistent with the subsequent loss of $CHCl_3$ observed as effervescence in the open capillary. The second endotherm in the DSC begins at 451 K and reaches a maximum at 362 K, consistent with the second melting point observed at 448–451 K in the open capillary after the sample had resolidified following the initial melting and effervescence. In the TGA, a weight loss of 18.6% was observed near 413 K, consistent with the loss of exactly 1 equiv of $CHCl_3$ per molecule of (2), immediately following the initial melting of the crystal at 405–408 K. The 1:1 stoichiometry of the chloroform solvate is also consistent with the integration of the ^{1}H NMR peak at 8.32 p.p.m. in DMSO-d_6, as listed in §2. NMR data were collected on a Varian Gemini-300 NMR spectrometer at 300 MHz. Spectra and more details of TGA, DSC and NMR spectra are given in the supporting material.[2]

3. Results and discussion

3.1. Basic structure

Recrystallization of (2) from chloroform yielded well formed crystals suitable for single-crystal diffraction. After

---

[1] Refined ratios in *Pna*2_1 fluctuated a few percent around 0.50 [*e.g.* 0.535 (5):0.465 (5)], depending on the exact model and set of restraints that needed to be used owing to the high correlation of parameters in *Pna*2_1.
[2] Supplementary data for this paper are available from the IUCr electronic archives (Reference: RY5022). Services for accessing these data are described at the back of the journal.

data collection, systematic absences indicated either centro-symmetric *Pnma* or noncentrosymmetric polar *Pna2₁* space groups. Initial structure solution and refinement in *Pnma*, however, did not reveal a well defined single molecule. Only a solvate chloroform molecule and one dimethoxy benzene unit were readily discernable; the remainder of the structure appeared severely disordered. A close analysis of the data pointed towards whole-molecule disorder of the organic molecule, which, while itself not being mirror symmetric, is located in the solid state on a crystallographic mirror plane. The whole-molecule disorder of the structure seems to be possible because the two enantiomers are coincidentally spatially sufficiently similar to be interchangeable within the crystal, as will be described in detail in the following sections.

Refinement of the structure in *Pnma* taking disorder into account was then straightforward (see §2.2.2). An *ORTEP*-style plot of one single molecule is given in Fig. 1, and a view of the expanded asymmetric unit showing the disorder is shown in Fig. 2.

A substantial portion of the molecule does actually exhibit approximate chemical mirror symmetry. Within the backbone – consisting of substituted aromatic rings, methylene bridges and the C—N unit of the amide – the symmetry is only broken by the positions of the N and C atoms of the amide bridge. The steric demands of the two alternative orientations are very similar with the only significant differences being introduced by the functionality of the *N*-acetyl amide unit. Application of the mirror plane on the molecule as a whole inverts this asymmetric group and converts its *N*-acetyl unit into the nearly isosteric macrocyclic amide keto moiety. The acetyl methyl groups, which are located almost on the mirror plane, do not introduce any significant differences in spatial demand for the two orientations. The acetyl O atom, however, has a higher steric demand than its counterpart on the other side of the molecule – the O atom of the lactam keto group. When inverted, the acetyl group extends outwards further by about
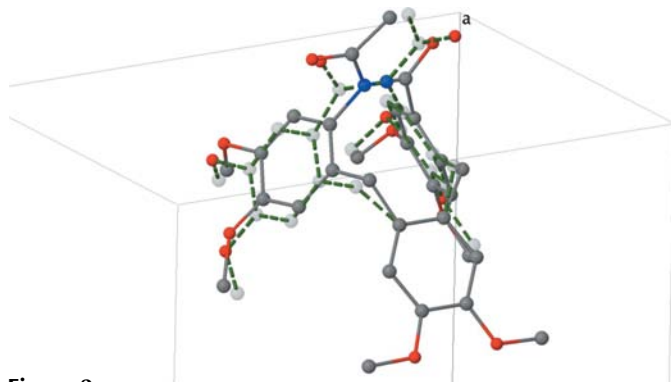
the length of the double bond of the acetyl C=O group (*i.e.* ∼ 1.2 Å). In order for both orientations of the molecule to still fit the same spatial region, each of the mirror-imaged *N*-acetyl amide groups has to shift by about half this distance towards the mirror plane. This shift of the atoms positioned away from the ideal mirror symmetry is most pronounced for the section of the molecule surrounding the *N*-acetyl amide group and slowly coalesces when reaching the opposite end of the molecule. Thus, the dimethoxybenzene unit furthest away from the *N*-acetylamide exhibits exact mirror symmetry, as does the solvate chloroform molecule (Fig. 2).

The acyl and keto functionalities of the *N*-acyl amide unit in the structure are coplanar and the unit as a whole consists of a conjugated imide group. The r.m.s. deviation of its constituent atoms – the *N*-acyl lactam atoms and the *ipso* carbon atoms of the adjacent phenyl rings – from its least-square plane is only 0.113 (4) with the largest individual deviation being just 0.170 (4) for the lactam oxygen atom O4. The plane of the *N*-acyl lactam group is basically perpendicular to those of the adjacent phenyl rings with dihedral angles of 82.7 (3) and 88.1 (3)°, respectively.

The 10-membered ring of (2) as a whole presents a cavity in the shape of a 'pinched bowl'. In the case of (2) the void within the bowl is filled by the *N*-acyl-lactam group of a neighbouring molecule and part of a chloroform molecule that both reach into this cavity (Fig. 3) forming stacked columnar assemblies along the *a* axis of the unit cell. The stacking of conical molecules in smectic assemblies is of interest in the preparation of liquid crystals (Sawamuru *et al.*, 2002; Kato *et al.*, 2006, and references therein). Native CTV typically forms crystalline clathrates with small molecules wherein the guests are located in channels between pillars of stacked CTV molecules
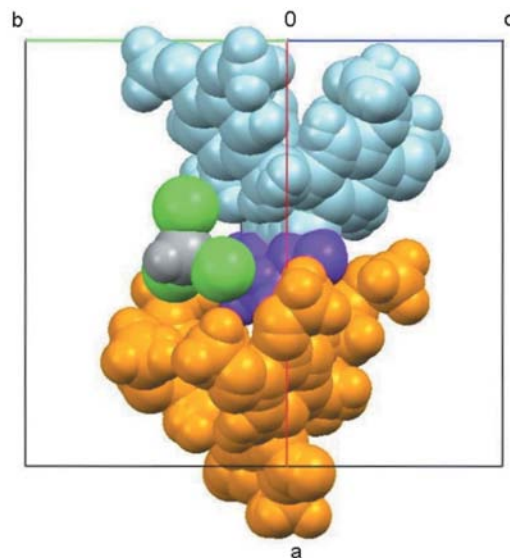
Figure 2
Ball-and-stick-style enhanced figure showing the whole-molecule disorder. To view the interactive figure online access http://submission.iucr.org/jtkt/serve/z/YpTnfhHJJnjiQCre/zz0000/0/. The chloroform solvate molecule is omitted for clarity. C atoms belonging to the second orientation of the molecule (created by the crystallographic mirror operation) are drawn in a lighter shade of gray; bonds within this moiety are indicated by dashed green lines. H atoms are omitted for clarity.

Figure 3
Spacefill representation showing how the *N*-acyl-lactam moiety (purple) and the solvate chloroform molecule reach into the conical cavity of a neighbouring molecule (gold). For better visibility the 'spacefill radii' of the atoms are set to 70% of the respective van der Waals radii. Both alternative orientations of the molecule are displayed. The view is perpendicular to the *a* axis and down the *b–c* diagonal of the unit cell.

(Steed *et al.*, 1996; Hyatt *et al.*, 1980). Extended-arm cavitands derived from CTV may also form stacked pillars of the bowl-shaped molecules (Hardie *et al.*, 2004). Hardie has specifically observed racemic CTV-derived host molecules with alternating chiralities stacked within a column in the racemic crystal (Ahmad & Hardie, 2006).

In solution CTV and its derivatives may undergo an interconversion between the crown conformer such as found here in the solid state and the alternative saddle conformer (Zimmermann *et al.*, 2004). Umbrella-like inversion of the chiral bowl-shaped lactam would lead to inversion of stereochemistry, and racemization of an enantiopure derivative. The barrier to interconversion for the parent (nine-membered ring) CTV was determined by Collet using enantiopure CTV-d_9 to be 111 kJ mol^{-1} (Collet, 1987). We suspect that the barrier to interconversion in the ten-membered ring lactam system may be similar, and we are currently resolving the lactam to explore potentially enantioselective host–guest chemistry, and to determine the barrier to interconversion of the enantiomers. NMR spectra of (2) in CDCl$_3$, however, indicate no interconversion of saddle and crown isomers here. Confirming the presence of the rigid crown conformation, the ^{1}H NMR shows, in addition to six unique aryl C—H protons and six unique methoxy singlets, two *AB* quartets between 3.4 and 4.3 p.p.m. with a strong geminal coupling of 14.7 Hz. The acetyl singlet resonates at 2.74 p.p.m., deshielded ~ 0.5 p.p.m. downfield from a typical imide methyl group because of the anisotropy induced by the macrocyclic amide carbonyl. Amide rotamers are observed in CDCl$_3$ in a ratio of 4:1, presumably favouring the *syn* coplanar conformation over the *anti* conformation, whereas amide rotamers are not observed in the more polar DMSO-d_6 solvent. The crystal structure confirms the *syn* coplanar conformation of the acyl moiety in the solid, placing the methyl group within the deshielding cone of the amide carbonyl, at least in the crystalline state. This overall rigidity of (2) may be attributed to the lactam linker in (2), which is significantly more rigid than its carbocyclic [2.1.1]orthocyclophane analogue recently prepared by Yamato *et al.* (2001), which exists as an equilibrium mixture of crown, *syn*-saddle and *anti*-saddle conformers. Yamato *et al.* (2001) reported the crystal structure of the highly flexible *anti*-saddle conformer – not the rigid 'bowl-shaped' crown conformer as observed for macrocycle (2).

The DSC of *N*-acetyl derivative (2) reveals two separate endothermic events. The first endotherm occurs at 421 K and is consistent with melting of the crystal and concomitant loss of CHCl$_3$. A second endotherm at 462 K is consistent with the second melting point observed by melting-point determination in a capillary. Weight loss near 413 K observed in the TGA is consistent with the loss of one molecule of CHCl$_3$ per molecule of (2) from the melted crystal. The sintering that we had observed visually in the capillary melting-point measurement at 389–391 K, which we considered may reflect a possible transition to a liquid crystalline phase, was not apparent in the DSC. Consistent with the visual melting point, the effervescence due to boiling off the chloroform occurs as the crystal melts, as the chloroform is released from the crystal

lattice, and thus does not appear as a separate endotherm in the DSC. We considered that we might observe an exotherm for resolidification of the material after the initial melting plus effervescence, but the exotherm is presumably obscured by the more energetic endotherm from the loss of solvent.

3.2. Two-dimensional solid solution racemate built of infinite racemic columnar assemblies

While the structure of the individual molecule as well as the apparent disorder within the crystal initially attracted our interest, we then turned our attention to the unique arrangement of the individual units within the crystal structure as a whole. The space group that (2) crystallizes in is centrosymmetric. Asymmetrically substituted calixarene-like molecules such as (2) are, however, planar chiral and thus averaged over the crystal as a whole the compound must be a racemate with a one-to-one ratio of enantiomers. The vast majority of crystalline racemic mixtures consist of a racemic compound where both enantiomers in the unit cell are related by a crystallographic inversion or mirror symmetry. Racemates may also be conglomerates (Kondepudi & Crook, 2005), containing pure crystals of the two enantiomers mechanically intermixed with one another as in the famous case of sodium ammonium tartrate manually resolved by Pasteur. Lastly, crystalline racemates may be solid solutions, with random dispersion of the two enantiomers throughout the crystal (Jacques *et al.*, 1991). Solid solutions are rare (Huang *et al.*, 2006), but it has been suggested that chiral molecules with a pseudo-element of symmetry are more likely to crystallize as solid solutions (Chion *et al.*, 1978). Similarly, pseudo-symmetric diastereomers or enantiomers that are similar in shape to a sufficient extent are more likely to crystallize as solid solutions (Barabas *et al.*, 2000). Strictly speaking, however, crystalline (2) does not belong to any of these three classes. As will be described in detail in the following sections (2) seems to have some properties of a classical racemate, with crystallographic inversion symmetry within individual columns consisting of molecules of alternating chirality (two-dimensional), yet it is made up of a solid solution with a statistical distribution of the two enantiomers between adjacent parallel columns.

The individual molecules of (2) are azacyclophane derivatives containing a cavity formed by three constituent phenyl moieties. The cavity is in turn filled by the *N*-acyl-lactam group of a neighbouring molecule and part of a solvate chloroform molecule. Neighbouring molecules along the *a* axis are in this way interlocked with one another and form infinite chains or columnar assemblies throughout the crystal. The connection between adjacent molecules along theses chains is, in part, facilitated by a number of medium-strength intermolecular interactions. There are no acidic H atoms (aside from the chloroform C—H), so there are no classical hydrogen bonds. There are, however, a range of weak non-classical C—H$\cdots$O hydrogen bonds and also several C—H$\cdots\pi$ contacts within the cavity. While these forces are individually relatively weak, in the absence of other stronger interactions they constitute a

large part of the attractive forces between neighbouring molecules (van de Velde *et al.*, 2004). The exact nature of these interactions is complicated by the whole-molecule disorder. A close analysis of all potential interactions within the chains along the axis, however, reveals that there is only one rational arrangement of the disordered molecules within each chain, and that this arrangement consists of alternating molecules with opposite chirality but with the *N*-acyl-amide units all pointing towards the same side of the chain, as shown in Fig. 4. This is most easily shown for the C—H···O contacts (Table 2) which within each chain dominate the interactions between neighbouring molecules: The more protruding acyl oxygen atom O5 induces a slight rotation of the neighbouring molecule around its centre of gravity *via* a C—H···O bond. This rotation allows its methoxy group on the other side of the molecule to approach the lactam keto O4 atom of the other molecule to form two other medium–strong C—H···O bonds. For an arrangement with alternating D and L molecules, as in Fig. 4, the most prominent C—H···O interactions that contribute to the binding within each cavity have H···O distances of 2.36 and 2.65 Å (for C13A—H13E···O5^v and C13—H13C···O4^v, respectively; Table 2). This is well within the usual range found for this kind of weak hydrogen bond-like interaction. Placing two molecules with the same sense of rotation in adjacent positions along the chains, however,
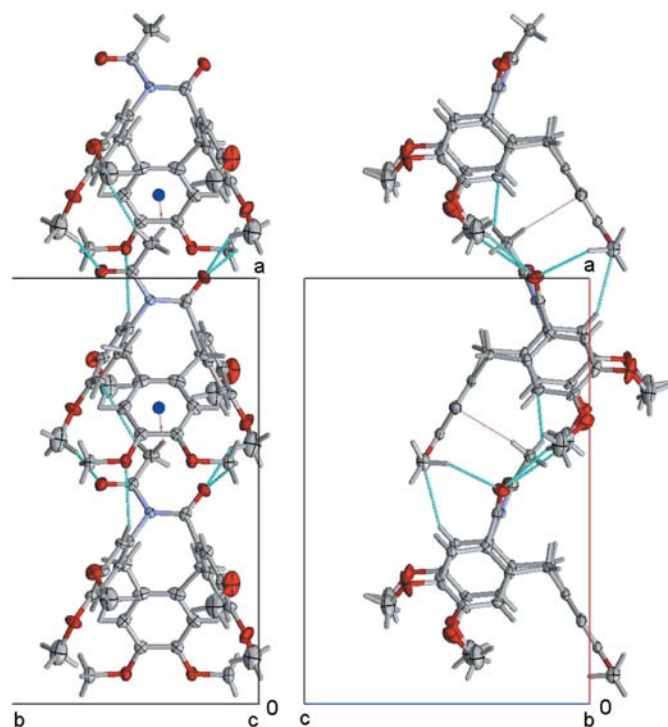

Figure 4
ORTEP-style representation showing a section of the columnar assembly along the *a* axis showing the intermolecular interactions. C—H···O and C—H···C interactions are represented by light blue dotted lines. Red dotted lines represent C—H···π bonds towards the centroid of an aromatic ring (displayed as a dark blue sphere). Displacement ellipsoids are at 50% probability; H atoms are drawn as capped rods. View down (*a*) the *c* axis and (*b*) the *b* axis (right). This figure is in colour in the electronic version of this paper.

Table 2
C—H···O intermolecular interactions (Å, °).

D—H···A	D—H	H···A	D···A	D—H···A
C3A—H3A···O3^i	0.95	2.67	3.497 (8)	146
C18—H18C···C6A^{ii}	0.98	2.79	3.606 (13)	141
C15—H15···O3^{iii}	1.00	2.35	3.220 (4)	145
C12A—H12D···O2A	0.98	2.40	2.968 (19)	116
C18—H18A···Cg1^{iv}	0.98	2.63	3.496	148
C14—H14A···O4^v	0.98	2.68	3.381 (7)	129
C13A—H13E···O5^v	0.98	2.36	3.271 (14)	155
C13—H13C···O4^v	0.98	2.65	3.466 (14)	141
Selected C—H···O bonds in the alternative (not realised) setting with enantiopure chains along **a**				
C13A—H13E···O4^{vi}	0.98	2.95	3.880 (13)	159
C13—H13C···O5^{vi}	0.98	2.10	2.862 (15)	133

Symmetry codes: (i) $x + \frac{1}{2}, -y + \frac{1}{2}, -z + \frac{1}{2}$; (ii) $x + \frac{1}{2}, y, -z + \frac{1}{2}$; (iii) $x + \frac{1}{2}, y, -z + \frac{3}{2}$; (iv) $-x, y + \frac{1}{2}, -z$; (v) $x - \frac{1}{2}, y, -z + \frac{1}{2}$; (vi) $x - \frac{1}{2}, -y + \frac{1}{2}, -z + \frac{1}{2}$; (vii) $x, \frac{1}{2} - y, z$. Ring centroid Cg1 based on the atoms C9, C10, C11, C9^{vii}, C10^{vii}, C11^{vii}.

would enforce a very short C—H···O contact of 2.10 Å for C13—H13C···O5^{vi} and a second main C—H···O contact, C13A—H13E···O4^{vi}, would be stretched to 2.95 Å. Furthermore, the assigned arrangement with alternate D and L molecules also avoids a close H···H contact of 1.94 Å between H18C and H13C (the contact between H18C and H13E is 2.411 Å). A similar analysis for the C—H···π contacts leads to the same conclusion: that enantiomers must alternate within a given column (Table 2).[3]

Barring a discontinuity along the chain each column parallel to the *a* axis thus consists of infinite chains of alternating D and L molecules with all *N*-acyl-lactam units within one chain pointing to the same side of the chain, and all O atoms (C—H···O) consistently binding to the same methoxy group (C13—H13C and C14—H14a to O4^v and C13A—H13E to O5^v). The next molecule in the chain is, however, mirror imaged: it is predicted by the exact application of the 'a' glide plane of the *Pnma* cell. This means each column is a perfect racemate by itself with an infinite D–L–D–L–D–L motif.

Do neighbouring chains influence each other's arrangement of the D and L molecules? Any D–L arrangement of neighbouring chains that is not random at least within large domains of the crystal would have to result in the disappearance of the disorder and thus of the mirror plane in the *Pnma* setting. This would lead either to a change of the cell parameters by a transformation of the point group to translational symmetry – a possibility that can be readily rejected on the basis of the diffraction patterns – or to the formation of a crystal with the lower symmetry and non-centrosymmetric space group *Pna*2$_1$. However, refinement in this space groups led – even considering racemic twinning – to the same type of disorder as observed in *Pnma*. An analysis of the packing of neighbouring chains leads to a similar conclusion. Neighbouring chains created by the *n* glide plane are pointing in opposite directions

---

[3] This analysis is nonetheless complicated by the disorder of the molecules and one runs the risk that inaccurately positioned atoms might lead to erroneous conclusions. The atom positions were, however, refined without any positional restraints. Further, based on bond-distance considerations no reasonable reassignment of atom positions to the other moiety is possible.

and are interlocked with each other *via* the extending methoxy groups and the solvate chloroform molecules. Thus, one would expect them to be unable to shift against each other in the solid state as this would involve shifting an entire column through the whole crystal. Therefore, any alignment of either D or L molecules in neighbouring chains has to be established throughout the crystallization process. Unlike within a given chain there seems to be no preferential set of intermolecular forces between neighbouring columns. This leaves a random arrangement of chains with respect to each other as the only possible arrangement. In this sense the crystal may be characterized as a *solid solution of chiral molecules consisting of racemic columnar assemblies*. In planes perpendicular to the *a* axis the distribution of D and L molecules thus appears to be random, and these planes thus each form a layer that could be viewed as a two-dimensional solid solution. However, along the *a* axis the enantiomers are alternating within each chain as in a classic racemic crystal where adjacent enantiomers in the unit cell are related by crystallographic inversion or mirror symmetry.

4. Summary and conclusions

The Beckmann ring-expanded CTV derived *N*-acetyl amide (2) was crystallized as a chloroform monosolvate as a two-dimensional solid solution of racemic columnar assemblies consisting of alternating enantiomers in a stacked-cup array, but with a random distribution of the columns within the crystal leading to whole-molecule disorder within the crystal. DSC and TGA analysis are consistent with open-capillary melting-point measurements of the crystalline solvate and expulsion of the chloroform solvent, followed by resolidification and a second melting event.

References

Ahmad, R. & Hardie, M. J. (2006). *Supramol. Chem.* **18**, 29–38.

Barabas, O., Menyhard, D. K., Bocskei, Z., Simon, K., Kiss-Ajzert, I., Takacs, K. & Hermecz, I. (2000). *Tetrahedron Asymmetry*, **11**, 4061–4070.

Bruker (2007). *Apex*2, Version 2.1–4. Bruker AXS Inc, Madison, Wisconsin, USA.

Bruker (2000–2003). *SHELXTL*6.14. Bruker AXS Inc, Madison, Wisconsin, USA.

Burlinson, N. E. & Ripmeester, J. A. (1984). *J. Inclusion Phenom.* **1**, 403–409.

Chion, B., Lajzerowicz, J., Bordeaux, D., Collet, A. & Jacques, J. (1978). *J. Phys. Chem.* **82**, 2682–2688.

Collet, A. (1987). *Tetrahedron*, **43**, 5725–5759.

Collet, A. (1996). *Comprehensive Supramolecular Chemistry*, edited by J. L. Atwood, J. E. D. Davies, D. D. MacNicol, F. Vögtle & J. M. Lehn, Vol. 6, pp 281–303. Pergamon Press: Oxford, England.

Hardie, J. J., Mills, R. M. & Sumby, C. J. (2004). *Org. Biomol. Chem.* **2**, 2958–2964.

Huang, J., Chen, S., Guzei, I. A. & Yu, L. (2006). *J. Am. Chem. Soc.* **128**, 11985–11992.

Hyatt, J. A., Duesler, D. Y., Curtin, D. Y. & Paul, I. C. (1980). *J. Org. Chem.* **45**, 5074–5079.

Jacques, J., Collet, A. & Wilen, S. H. (1991). *Enantiomers, Racemates and Resolutions* (reprint edition, reissued with corrections). Krieger Publishing Co.: Malabar, FL.

Kato, T., Mizoshita, N. & Kishimoto, K. (2006). *Angew. Chem. Int. Ed.* **45**, 38–68.

Kondepudi, D. K. & Crook, K. E. (2005). *Crystal Growth Des.* **5**, 2173–2179.

Lutz Jr, M. R., French, D. C., Rehage, P. & Becker, D. P. (2007). *Tetrahedron Lett.* **48**, 6368–6371.

Lutz Jr, M. R., Zeller, M. & Becker, D. P. (2007). *Acta Cryst.* E**63**, o3857–o3858.

Lutz Jr, M. R., Zeller, M. & Becker, D. P. (2008). *Tetrahedron Lett.* **49**, 5003–5005.

Sawamuru, M., Kawai, K., Matsuo, Y., Kanie, K., Kato, T. & Nakamura, E. (2002). *Nature (London)*, **419**, 702–705.

Sheldrick, G. M. (2008). *Acta Cryst.* A**64**, 112–122.

Steed, J. W., Zhang, H. & Atwood, J. L. (1996). *Supramolecular Chemistry*, **7**, 37–45.

Yamato, T., Sakaue, N., Tanaka, K. & Tsuzuki, H. (2001). *New J. Chem.* **25**, 434–439.

Velde, C. M. L.van de, Chen, L. J., Baeke, J. K., Moens, M., Dieltiens, P., Geize, H. J., Zeller, M., Hunter, A. D. & Blockhuys, F. (2004). *Crystal Growth Des.* **4**, 823–830.

Zimmermann, H., Tolstoy, P., Limbach, H.-H., Poupko, R. & Luz, Z. (2004). *J. Phys. Chem. B*, **108**, 18772–18778.